◆ Human Brain Mapping 33:2971–2983 (2012) ◆

Late Effects of High-Dose Adjuvant Chemotherapy on White and Gray Matter in Breast Cancer Survivors: Converging Results from Multimodal Magnetic Resonance Imaging

Michiel B. de Ruiter,[1,2,3]* Liesbeth Reneman,[2] Willem Boogerd,[4] Dick J. Veltman,[5,6] Matthan Caan,[2] Gwenaëlle Douaud,[3] Cristina Lavini,[2] Sabine C. Linn,[7] Epie Boven,[8] Frits S.A.M. van Dam,[1] and Sanne B. Schagen[1]

[1]*Department of Psychosocial Research and Epidemiology, Netherlands Cancer Institute, Amsterdam, The Netherlands*
[2]*Department of Radiology, Academic Medical Center, University of Amsterdam, Amsterdam, The Netherlands*
[3]*Department of Clinical Neurology, FMRIB Centre, University of Oxford, Oxford, UK*
[4]*Department of Neuro-oncology, Netherlands Cancer Institute, Amsterdam, The Netherlands*
[5]*Department of Psychiatry, VU University Medical center, Amsterdam, The Netherlands*
[6]*Department of Psychiatry, Academic Medical Center, University of Amsterdam, The Netherlands*
[7]*Department of Medical Oncology, Netherlands Cancer Institute, Amsterdam, The Netherlands*
[8]*Department of Medical Oncology, VU University medical center, Amsterdam, The Netherlands*

Abstract: The neural substrate underlying cognitive impairments after chemotherapy is largely unknown. Here, we investigated very late (>9 years) effects of adjuvant high-dose chemotherapy on brain white and gray matter in primary breast cancer survivors ($n = 17$) with multimodal magnetic resonance imaging (MRI). A group of breast cancer survivors who did not receive chemotherapy was scanned for comparison ($n = 15$). Neuropsychological tests demonstrated cognitive impairments in the chemotherapy group. Diffusion tensor imaging (DTI) with tract-based spatial statistics showed that chemotherapy was associated with focal changes in DTI values indicative for reduced white matter integrity. Single voxel proton MR spectroscopy (1H-MRS) in the left centrum semiovale (white matter) showed a reduction of *N*-acetylasparate/creatine indicative of axonal injury. Voxel-based morphometry demonstrated a reduction of gray matter volume that overlapped with fMRI hypoactivation (as reported in a previous publication) in posterior parietal areas and colocalized with DTI abnormalities. Also, DTI correlated with 1H-MRS only in the chemotherapy group. These results converge to suggest

Additional Supporting Information may be found in the online version of this article.

Contract grant sponsors: The Netherlands Cancer Institute, The department of Radiology (Academic Medical Center of the University of Amsterdam).

*Correspondence to: Michiel B. de Ruiter, Department of Psychosocial Research and Epidemiology, Netherlands Cancer Institute, Plesmanlaan 121, 1066 CX Amsterdam, The Netherlands.
E-mail: mbderuiter@gmail.com

Received for publication 3 March 2011; Accepted 24 June 2011
DOI: 10.1002/hbm.21422
Published online 23 September 2011 in Wiley Online Library (wileyonlinelibrary.com).

that high-dose adjuvant chemotherapy for breast cancer is associated with long-term injury to white matter, presumably reflecting a combination of axonal degeneration and demyelination, and damage to gray matter with associated functional deficits. Hormonal treatment with tamoxifen may also have contributed to the observed effects, although results from other studies indicate that it is unlikely that tamoxifen is solely or largely responsible. Using this multimodality approach we provide for the first time insight into the neural substrate underlying cognitive impairments following systemic administration of cytotoxic agents many years after treatment. *Hum Brain Mapp 33:2971–2983, 2012.*

Key words: chemotherapy; magnetic resonance imaging; breast cancer; diffusion tensor imaging; proton MR spectroscopy; voxel-based morphometry; multimodal MRI; cognitive functioning; side effects

INTRODUCTION

Adjuvant chemotherapy increases the cure rate in patients with high-risk primary breast cancer and is nowadays administered in as many as 60% of patients below the age of 70. The term "adjuvant" refers to chemotherapy given after radical breast cancer surgery to eradicate occult disease. Breast cancer patients that have been treated with cytotoxic agents regularly report cognitive problems [van Dam et al., 1998; Schagen and Vardy, 2007; Shilling and Jenkins, 2007; Weis et al., 2009]. Cognitive deficits have been observed in neuropsychological studies even years after cessation of chemotherapy [Correa and Ahles, 2008; Wefel et al., 2008].

In general, the blood–brain barrier is believed to prevent cytotoxic agents from entering the brain. However, some agents, like 5-fluorouracil and thiotepa, cross the blood–brain barrier to some extent by diffusion [Sakane et al., 1999; Strong et al., 1986]. Several preclinical studies have consistently shown that commonly used cytotoxic agents (such as methotrexate and cyclophosphamide) administered systemically can disrupt cell division in brain regions critical for memory and learning [Mignone and Weber, 2006; Seigers et al., 2008, 2009, 2010]. Various chemotherapeutic agents, like 5-FU and cisplatin, have been found to damage myelin-forming oligodendrocytes and their precursor cells in mice [Dietrich et al., 2006; Han et al., 2008]. Indirect neurotoxic effects may also be induced, possibly through oxidative stress, vascular damage or immune response dysregulation [Ahles and Saykin, 2007].

In humans, few neuroimaging data are available on the potential effects of chemotherapy. Functional imaging studies suggest altered activation patterns in brain areas involved in cognitive functioning following conventional regimens [de Ruiter et al., 2011; Kesler et al., 2009; Silverman et al., 2007]. In a functional magnetic resonance imaging (fMRI) study from our group, we compared breast cancer survivors that had received high-dose adjuvant chemotherapy almost 10 years earlier with survivors for whom chemotherapy had not been indicated. We found a profound hyporesponsiveness of the posterior parietal cortex during a memory encoding and an executive functioning task, among other brain areas specific for the task at hand [de Ruiter et al., 2011]. Structural imaging studies using voxel-based morphometry (VBM) have reported volume reductions of white [Inagaki et al., 2007] and gray [Inagaki et al., 2007; McDonald et al., 2010] matter within 1 year after cessation of standard dosages of chemotherapy compared to non-chemotherapy receiving cancer patients. However, recovery over time of these reductions was also observed.

On a microstructural level, diffusion tensor imaging (DTI) is particularly sensitive to injury to white matter fibre tracts by measuring the diffusion of water. DTI enables the estimation of various parameters, such as fractional anisotropy (FA), a measure of the directionality of diffusion, and mean diffusivity (MD), which indexes the average amount of diffusion. Both FA and MD are determined by axial diffusivity (AD) and radial diffusivity (RD), reflecting the diffusion of water parallel and perpendicular to white matter tracts, respectively [Pierpaoli and Basser, 1996; Pierpaoli et al., 1996]. Although the biological basis of these measures is complex, decreases in AD are interpreted as axonal injury whereas increases in RD are linked to myelin injury [Budde et al., 2009; Song et al., 2002, 2005; Sun et al., 2006, 2008].

One DTI study has reported lower FA in the genu of the corpus callosum in 10 breast cancer patients that received chemotherapy (on average less than 2 years earlier) compared to healthy controls [Abraham et al., 2008]. In a recent study, several DTI parameters in breast cancer patients who received standard-dose chemotherapy (on average 4 months earlier, $n = 17$) with matched healthy controls ($n = 18$) were compared with breast cancer patients that had not received chemotherapy ($n = 10$) [Deprez et al., 2011]. A decreased FA in frontal and temporal white matter and increased MD in frontal white matter was found in patients that received chemotherapy. In addition, within areas of decreased FA and increased MD, increases in RD were found, suggesting that changes in FA and MD values might be due to demyelination.

Some investigators have used proton MR spectroscopy (1H-MRS) to investigate neurochemical indices of white matter quality, but failed to find effects of chemotherapy

on *N*-acetylaspartate (NAA), a marker of axonal viability [Brown et al., 1995, 1998; Stemmer et al., 1994]. High-field MRI, however, was not performed, which may have obscured relevant changes due to low signal-to-noise ratios.

In summary, fragmented evidence is available with respect to abnormalities in brain structure and function of breast cancer survivors that have received chemotherapy. Previous studies often lacked an adequate comparison group and were usually performed shortly after chemotherapy. In addition, these studies focused only on one imaging modality and are therefore not informative on the effect of chemotherapy on different parameters of brain morphology and function, and their mutual relationships.

In the present study, we used DTI to investigate microstructural white matter integrity in the abovementioned group of breast cancer survivors who had received high-dose chemotherapy almost 10 years earlier. These patients were compared with a group of breast cancer survivors that had not received chemotherapy, thus controlling for cancer history. We analyzed absolute and relative concentrations of NAA and Choline (Cho) in cerebral white matter, using 1H-MRS in the centrum semiovale. To examine possible relations with gray matter volume and function, we measured changes in gray matter volume by performing VBM and compared these results to our previous fMRI study in the same group [de Ruiter et al., 2011]. Correlation analyses were carried out to investigate whether DTI and 1H-MRS indices of white matter integrity were related. Finally, performance on cognitive tests on which the CT group differed significantly from the no-CT group was correlated with DTI values. We expected to find evidence of white matter pathology (e.g., axonal degeneration and/or demyelination) using DTI and 1H-MRS and aimed to explore its relation with gray matter volume and function. We further hypothesized that DTI measures would correlate with 1H-MRS measures providing multimodal indications of detrimental effects of chemotherapy on brain white matter. In summary, using this multimodality imaging approach, we aimed to provide further insight in the pathophysiology of (long-term) neurotoxic effects of cytotoxic agents on the living human brain.

MATERIALS AND METHODS

Participants

Participants were disease-free breast cancer survivors from the Antoni van Leeuwenhoek Hospital/Netherlands Cancer Institute and the VU University medical center. The current study was approved by the institutional review board of both institutes. The chemotherapy (CT) group consisted of survivors who were high-risk breast cancer patients with at least four tumour-positive axillary lymph nodes, but no evidence of distant metastases at the time of treatment. They had received adjuvant standard CT consisting of four cycles of FEC (5-fluorouracil, 500 mg/m^2, epirubicin, 90 mg/m^2, cyclophosphamide, 500 mg/m^2) followed by one cycle of high-dose CTC (cyclophosphamide, 6 g/m^2, thiotepa, 480 mg/m^2, carboplatin, 1600 mg/m^2), and autologous peripheral blood hematopoietic progenitor-cell transplantation rescue. Patients from this group were subsequently treated with tamoxifen (40 mg daily) for 3.8 $\pm$ 1.7 years. The no-CT group consisted of cancer survivors previously diagnosed with stage I breast cancer that had not received any systemic therapy, except for one patient who was treated with tamoxifen for 5 years. All participants had undergone surgery and locoregional radiation therapy.

Exclusion criteria were: presence of metastatic disease or relapse, neurological and/or psychiatric symptoms or use of medication that might lead to deviant test results, alcohol and/or drug abuse and contraindications to undergo MR imaging. Written informed consent was obtained from all participants according to institutional guidelines.

Nineteen out of 23 eligible cancer survivors constituted the CT group. One of them turned out to be claustrophobic at the experimental session and for another survivor DTI and MR-S scans were corrupt. Thus, 17 out of 23 (73.9%) eligible cancer survivors constituted the CT group. Moreover, 15 out of 28 eligible cancer survivors (53.6%) constituted the no-CT group. Decliners in both groups did not differ from participants with respect to age, estimated IQ (based on an earlier assessment) or the presence of cognitive complaints. For more details on subject attrition see De Ruiter et al., 2011.

Self-Report Measures and Cognitive Tests

Health-related quality of life was assessed with the European Organization for Research and Treatment of Cancer (EORTC) Quality of Life Questionnaire-C30 [Aaronson et al., 1993] and anxiety and depressive symptoms were assessed with the Hopkins Symptoms Checklist-25 [Hesbacher et al., 1980]. To assess demographic variables and the occurrence of cognitive complaints, a 30-min structured telephone interview was held before including subjects in the study [Schagen et al., 1999]. During the experimental session, the Dutch Adult Reading Test was administered to obtain a measure of premorbid IQ [Schmand et al., 1992]. Also, seven neuropsychological tests yielding 16 test indices were administered. In addition, three cognitive paradigms were administered during fMRI sessions, specifically tapping cognitive functions that seem to be affected by chemotherapy [Vardy et al., 2008] (see Supplementary material and de Ruiter et al., 2011). Only tests that yielded significant group differences are reported here, because they were used for correlation with DTI parameters.

Experimental Procedure

The experimental procedure lasted ~2.5 h. Neuropsychological tests and questionnaires were completed (1 h

and 15 min). After a 30-min break, the MRI scanning session took place (1 h). Participants lay supine in the scanner and wore ear pads and a headphone to reduce scanner noise. The headphone was attached to a microphone, enabling communication with the experimenter in-between scan acquisitions. The order of scan acquisition was: fluid-attenuated inversion recovery (FLAIR), T1 weighted scans (T1W), fMRI (Flanker), DTI, fMRI (ToL), 1H-MRS, fMRI (paired associates).

Magnetic Resonance Imaging

Imaging data were obtained at the Academic Medical Center in Amsterdam, using a 3.0 T Intera full-body MRI scanner (Philips Medical Systems, Best, The Netherlands) with a phased array SENSE 6-channel receiver head coil. An axial FLAIR scan (TR/TE/TI = 11,000/100/2600 ms, FOV 230 × 230 mm, 27 slices, voxel size 0.9 × 1.20 × 5.0 mm, slice gap 0.5 mm) was acquired to score white matter abnormalities with the visual rating scale of Fazekas (range 0–3) [Fazekas et al., 1987]. All ratings were performed by a neuroradiologist (L. R.) blind to the clinical data. A sagittal 3D spoiled gradient echo (T1W, TR/TE = 9/3.53 ms, FOV 232 × 256 mm, 170 slices, voxel size 0.91 × 1.0 × 1.0 mm) was acquired for anatomical reference and VBM. DTI was acquired along 16 nonlinear and 16 antipodal directions (TR/TE = 4863/94 ms, FOV 230 × 230 mm, 38 slices, voxel size 2.05 × 2.05 × 3.0 mm, diffusion weighting parameter b: 1000 s/mm^2), covering the entire brain except for the cerebellum in some participants. Eddy current-induced morphing was corrected by a two-dimensional affine registration of the diffusion-weighted images to the average of four b_0 images [Mangin et al., 2002]. DTIFit within the FMRIB Diffusion Toolbox (part of FSL [Smith et al., 2004]) was used to fit a diffusion tensor model to the data at each voxel. Then, FA, MD, axial diffusivity (AD, λ_1) and radial diffusivity [RD, $(\lambda_2 + \lambda_3)/2$] maps were calculated. Tract-based spatial statistics (TBSS, also part of FSL [Smith et al., 2006]) was used to perform voxel-wise comparisons of DTI-parameters on "skeletonized" data. TBSS allows better alignment of FA images from multiple subjects for subsequent voxelwise analysis, and avoids non-arbitrary spatial smoothing. First, FA maps were nonlinearly registered to an FA template (FMRIB58_FA) and averaged. This mean FA map was thinned to create an FA skeleton. Each participant's FA data were then projected onto the mean skeleton by searching perpendicularly from the skeleton for maximal FA values and were thresholded at FA > 0.2. Next, MD, AD, and RD values from the same voxels were also mapped onto the skeleton.

Single voxel 1H-MRS was acquired in the left centrum semiovale. There are two very pragmatic reasons for this: it is a region of the brain that contains a lot of white matter, which facilitates placement of the 1H-MRS voxel, without contamination by gray matter, or CSF from the ventricles. It therefore is a region that gives a good signal-to-noise ratio. We chose the left side of the brain because it is usually conceived as the part of the brain that is predominant in cognitive functioning. We used a fully automated point resolved spectroscopy (PRESS) sequence including global shimming (mean voxel size = 10.7 ml, TR/TE = 2000/35–40 ms, NEX = 64). The sum of NAA and *N*-acetylaspartylglutamate (NAAG) was used because it provides more reliable estimates than NAA alone. Similarly, for Cho, the sum of the metabolites glycerophosphoryl-choline (GPC) and phosphocholine (PCH) was used. Spectra were analyzed using LCModel [Provencher, 1993]. Only spectra with a water peak full width at half maximum (FWHM) of less than 10 Hz and only metabolites with good fitting quality (SD < 15%) were included in the analysis, i.e., NAA + NAAG, Cr, and Cho. Concentrations of NAA +NAAG, Cho, and Cr were estimated and expressed in institutional units (IU) allowing direct comparison between spectra acquired on the same system. In addition, (NAA + NAAG)/Cr and Cho/Cr as provided by LC Model were obtained. Spectra were not acquired for one participant of the no-CT group due to time constraints. Water peak with FWHM exceeded 10 Hz in one subject from the CT group (0.107), but was included because of an acceptable SD < 15% for the metabolites. Therefore, 17 (CT group) and 14 (no-CT group) subjects were left for analyses of spectra.

"Optimized" VBM using FSL tools [Smith et al., 2004] was used to assess local volume differences in gray matter between groups. The T1W image was first skull-stripped and segmented into gray matter. Then, a left-right symmetric study-specific gray matter template was built from the gray matter segmentations of 15 no-CT cancer survivors and 15 out of 17 CT survivors (random selection) by nonlinear registration to the gray matter ICBM-152 template. Then, all 32 gray matter images were nonlinearly normalized onto the study-specific template. A voxel-wise adjustment of the warped images was applied to compensate for the amount of contraction or enlargement by dividing each voxel by the Jacobian of the warp field. Finally, the gray matter volume images were smoothed with an isotropic Gaussian kernel with a sigma of 3 mm (7 mm FWHM).

fMRI analyses were carried out in SPM5 as described previously by our group [de Ruiter et al., 2011]. In that study, blood oxygenation level dependent (BOLD) activation during two cognitive tasks, the paired associates and the Tower of London (ToL), were measured (the Flanker test did not elicit reliable task-related activation). During both tasks, the CT-group showed bilateral hyporesponsiveness of the posterior parietal cortex, in particular for the paired associates task. For illustrative purposes, group differences during the paired associated task were overlaid to allow for comparisons with our current DTI and VBM analyses. Data from one survivor from the CT group could not be obtained due to severe visual impairment. Therefore, 16 (CT group) and 15 (no-CT group) subjects were

left for fMRI analyses. Task-specific fMRI effects did not reveal additional effects in the vicinity of VBM or DTI effects.

Statistical Analysis

Demographic variables, self-reported measures, cognitive performance data, Fazekas ratings, and MR spectra were analyzed with SPSS 15.0 (SPSS Inc., Chicago, IL). Demographic and clinical data were analyzed by two-tailed independent-samples *t*-tests and χ^2-tests. MR spectra were analyzed with analysis of covariance (ANCOVA), including age as a covariate. Performance on the neuropsychological tests and fMRI paradigms was also analyzed with ANCOVA, including age and estimated IQ as covariates. ANCOVAs were run on the 16 raw neuropsychological test scores separately. For the number of tests in which participants showed impairments, a repeated measures ANCOVA with factor Time was incorporated (including a test interval within 2 years after chemotherapy and a test interval almost 10 years after chemotherapy or comparable intervals for the no-CT group). For the fMRI tasks, separate analyses were run for performance and RT. For the Flanker task, a repeated measures ANCOVA was run with the factor congruency (three levels: congruent, perceptually incongruent, and incongruent).

Mean whole-brain skeletonized DTI values (FA, MD, AD, and RD) were extracted to obtain mean DTI values across the white matter skeleton and tested in SPSS with age as covariate. In addition, the *randomize* program within FSL was used to perform permutation-based nonparametric inference (5000 permutations) on the DTI data within a general linear model framework [Nichols and Holmes, 2002] to investigate group differences in specific white matter regions (voxelwise analysis). Again, group differences were assessed for FA, MD, AD, and RD using age as a covariate.

DTI parameters were correlated with 1H-MRS and cognitive performance. All analyses were run separately for the two groups. MD was used because, in the present study, it was the most sensitive DTI parameter as indicated by TBSS (most widespread group differences across the white matter skeleton). For assessing correlations of DTI with 1H-MRS, first, a region-of-interest (ROI) approach was used. In addition to MD, AD, and RD were also used to clarify the pathophysiology of chemotherapy-induced neurotoxicity as indicated by different imaging modalities. Mean MD, AD, and RD values for the skeletonized white matter that was located within the 1H-MRS voxel in the centrum semiovale were correlated with NAA/Cr and NAA in SPSS. In addition, MD values were correlated with NAA/Cr and NAA in *randomize* to reveal specific white matter regions across the white matter skeleton that correlated with NAA/Cr and NAA. Subsequently, mean values across significant clusters were extracted to calculate correlation coefficients in SPSS. A similar approach was followed for correlation of MD with cognitive performance: mean MD values across significant clusters (as provided by *randomize*) were extracted to calculate correlation coefficients with cognitive performance in SPSS.

For all DTI analyses including correlation analyses, cluster-based thresholding at $P < 0.05$, fully corrected for multiple comparisons, was performed by using the null distribution of the maximum cluster size. Only performance on cognitive tests in which the CT group differed significantly from the no-CT group was correlated with DTI measures. For calculation of correlation coefficients in SPSS, significance was set at $P < 0.05$, uncorrected. The ICBM-DTI-81 atlas was used for anatomical reference [Mori et al., 2008]. *Randomize* was also used for the VBM analyses, again incorporating age as a covariate and applying cluster-based thresholding at $P < 0.05$, corrected for multiple comparisons.

TABLE I. Demographic and clinical characteristics of the study population

	CT group ($n = 17$)	No-CT group ($n = 15$)	P value
Age	56.5 ± 5.1	58.2 ± 5.8	0.53
Estimated IQ (NART)	99.8 ± 18.6	100.7 ± 17.3	0.89
Years since surgery	9.9 ± 0.8	9.2 ± 0.5	0.005
Years since chemotherapy	9.5 ± 0.8	NA	NA
EORTC QLQ-C30			
Global quality of life	80.4 ± 11.8	81.1 ± 16.2	0.89
Fatigue	26.8 ± 14.7	23.0 ± 19.5	0.53
HSCL-25 anxiety	10.6 ± 6.7	13.6 ± 13.5	0.45
HSCL-25 depression	12.0 ± 8.0	15.7 ± 19.2	0.50
Cognitive complaints			
Concentration, *n* (%)	7 (41.2%)	6 (40%)	0.95
Memory, *n* (%)	10 (58.8%)	3 (20%)	0.03
Thinking, *n* (%)	0 (0%)	1 (6.7%)	0.28
Language, *n* (%)	3 (17.6%)	6 (40%)	0.16

Values indicate mean ± SD unless indicated otherwise.
CT, chemotherapy; NART, Dutch version of the National Adult Reading Test; EORTC QLQ-C30, European Organization for Research and Treatment of Cancer health-related Quality-of-Life Questionnaire: scores range from 0 to 100; HSCL-25, Hopkins Symptom Checklist-25: scores range from 0 to 100, higher score indicates higher levels of anxiety and depression; NA, not applicable.

RESULTS

Patient Characteristics

The CT group and no-CT group did not differ significantly with regard to age and estimated IQ. Cancer survivors were assessed on average 9.55 ± 0.73 years after surgery. No significant differences were detected between the CT and the no-CT patients with regard to measures for quality of life, anxiety, and depression. More breast cancer survivors who received CT complained of memory problems than those who did not receive CT (Table I).

TABLE II. Cognitive tests indices showing significant group differences

	CT group ($n = 17$)*	No-CT group ($n = 15$)	P value
Mean % impairment on 16 neuropsychological test indices	11.6 ± 12.7	5.2 ± 4.5	0.04
Word fluency professions	16.9 ± 3.8	19.9 ± 4.3	0.03
Tower of London mean % correct	72.1 ± 14.6	82.8 ± 12.3	0.04
Tower of London reaction time (s)	8.8 ± 3.1	11.9 ± 3.8	0.02
Flanker test mean % correct	95.0 ± 2.7	97.0 ± 2.2	0.03

Values indicate mean ± SD. For details, see Supplementary Material.
CT, chemotherapy.
*For the Tower of London and the Flanker test, $n = 16$.

TABLE III. Fazakas ratings of white matter hyperintensities on FLAIR scans

	CT group ($n = 17$)	No-CT group ($n = 15$)	P value
Fazekas 0	6 (35.3%)	7 (46.7%)	0.76
Fazekas 1	9 (52.9%)	6 (40.0%)	
Fazekas 2	2 (11.8%)	2 (13.3%)	

Values indicate absolute numbers with percentage in parentheses.
CT, chemotherapy.
P value shows result of χ^2-test.

Cognitive Test Performance

Across two time-points (within 2 years after chemotherapy and almost 10 years after chemotherapy), the CT group was impaired on a significantly higher percentage of tests than the no-CT group [F (1, 28) = 9.36, $P < 0.05$]. No significant change in cognitive impairment occurred over time. With respect to the 16 raw neuropsychological test indices, only one significant group difference was found: the CT group scored worse on the Word fluency professions test [F (1, 28) = 5.42, $P < 0.05$]. On 13 out of the 15 remaining indices, the CT group performed numerically worse than the no-CT group (data not shown). For the Flanker test, the CT group committed significantly more errors than the no-CT group across test conditions, congruent, perceptually incongruent, and incongruent [F (1, 27) = 5.29, $P < 0.05$]. No other statistically significant effects involving the factor Group were found for accuracy, or for RT. For the ToL, the CT group performed significantly worse [F (1, 27) = 4.69, $P < 0.05$] and faster [F (1, 27) = 5.64, $P < 0.05$] than the no-CT group (Table II). No significant group differences were found for the paired associates test.

White Matter Hyperintensity Ratings

Fazekas ratings of white matter hyperintensities on FLAIR scans ranged between 0 and 2 for both groups and did not differ significantly as assessed with a χ^2-test (Table III).

DTI

Calculating mean DTI values across the entire white matter skeleton, the CT group showed a significant increase in MD and AD, and a borderline significant increase in RD ($P = 0.05$, Table IV). Performing voxel-wise permutation testing on the skeletonized data (TBSS), in addition, indicated significantly lower focal FA values (8.6% mean decrease) in the CT compared to the no-CT group in the left anterior corona radiata, left external capsule, left sagittal stratum (including inferior longitudinal fasciculus and inferior fronto-occipital fasciculus), and

TABLE IV. DTI parameters for entire white matter skeleton and for significant clusters within white matter skeleton as provided with tract-based spatial statistics (TBSS) at $P < 0.05$ corrected

	CT group ($n = 17$)	No-CT group ($n = 15$)	mm^3	Increase/Decrease	P value
Entire WM skeleton					
Fractional anisotropy	0.451 ± 0.015	0.456 ± 0.012	NA	−1.1%	0.18
Mean diffusivity ($\mu m/s^2$)	0.785 ± 0.021	0.770 ± 0.018	NA	+1.9%	0.02
Axial diffusivity ($\mu m/s^2$)	1.201 ± 0.019	1.184 ± 0.021	NA	+1.4%	0.02
Radial diffusivity ($\mu m/s^2$)	0.577 ± 0.024	0.564 ± 0.019	NA	+2.3%	0.05
TBSS Significant clusters					
Fractional anisotropy	0.539 ± 0.027	0.590 ± 0.018	2235	−8.6%	<0.001
Mean diffusivity ($\mu m/s^{2)}$)	0.808 ± 0.027	0.753 ± 0.019	8568	+7.3%	<0.001
Radial diffusivity ($\mu m/s^{2)}$)	0.549 ± 0.037	0.491 ± 0.019	4442	+11.8%	<0.001

Values indicate mean ± SD. P values correspond to ANCOVA results including extracted DTI parameters with age as covariate.
CT, chemotherapy; Nr, number; WM, white matter; NA, not applicable; TBSS, tract-based spatial statistics mm^3 indicates mm^3 of white matter skeleton that show significant differences between groups.

bilateral posterior thalamic radiation (including the optic radiation). No regions were found with significantly higher FA values in the CT than in the no-CT group. For MD, the effects were more widespread than for FA and significant increases (7.3% mean increase) in the CT compared to the no-CT group were present in the bilateral retrolenticular part of the internal capsule, bilateral posterior thalamic radiation (including the optic radiation), bilateral sagittal stratum (including the inferior longitudinal fasciculus and inferior fronto-occipital fasciculus), right posterior limb of the internal capsule, bilateral anterior corona radiata, bilateral superior corona radiata, bilateral superior longitudinal fasciculus and the body and genu of the corpus callosum. No significant MD decreases were found in the CT relative to the no-CT group. Finally, increases in RD (11.8% on average) in the CT-group compared to the no-CT group were present in similar regions as the decreases in FA but were more widespread and located in left anterior corona radiata, left external capsule, left sagittal stratum (including inferior longitudinal fasciculus and inferior fronto-occipital fasciculus), left retrolenticular part of the internal capsule, and bilateral posterior thalamic radiation (including the optic radiation), left posterior and left superior corona radiata. No significant RD decreases were found in the CT relative to the no-CT group (Table IV, Fig. 1). No significant group differences were found for AD with TBSS.

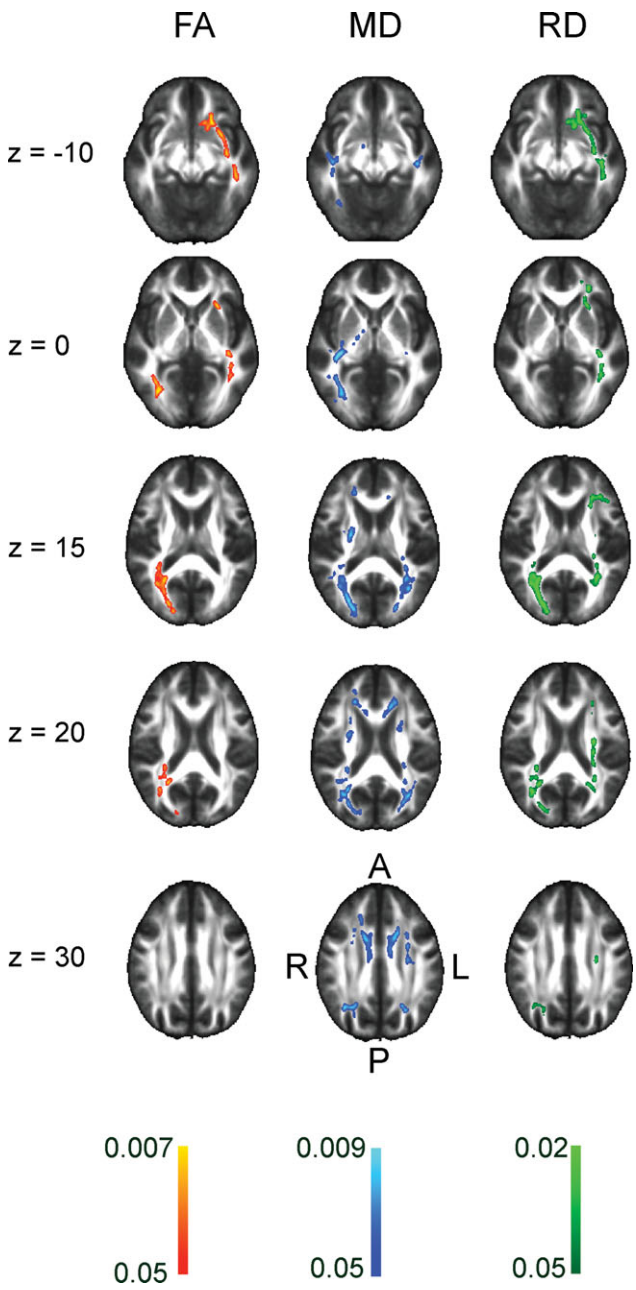

1H-MRS

No significant differences in absolute concentrations of NAA, Cho or Cr were found between groups. NAA/Cr, however, was significantly lower for the CT group than for the no-CT group. Cho/Cr was similar for both groups (Table V).

DTI and fMRI

To compare the DTI data with results of our previous fMRI study, maps reflecting increases in MD and RD in the CT versus to no-CT group were overlaid on the blood oxygenation level dependent (BOLD) contrast maps reflecting relative decreases in activation in the CT versus the no-CT group during the encoding phase of a paired associates memory test [de Ruiter et al., 2011]. Increases in MD and RD in white matter tracts in the posterior thalamic/optic radiation (bilateral for MD and in the right hemisphere for RD) were located adjacent to areas

Figure 1.

Group differences in DTI values between the chemotherapy (CT) group and the no-CT group. DTI data were analyzed with tract-based spatial statistics (TBSS) on "skeletonized" white matter. Cluster-based thresholding at $P < 0.05$ was applied, fully corrected for multiple comparisons. Areas of the white matter skeleton that show significant group differences are overlaid on a fractional anisotropy (FA) map, derived from the mean of the FA maps of all participants that have been normalized to standard MNI space. Significant clusters have been thickened for ease of visualization. Left panel shows regions where the CT group has a lower FA than the no-CT group. Middle panel shows regions where the CT group has a higher mean diffusivity (MD) than the no-CT group. Right panel shows regions where the CT group has a higher radial diffusivity (RD) than the no-CT group. See text for description of affected white matter tracts. Color bars show range of corrected *P* values. [Color figure can be viewed in the online issue, which is available at wileyonlinelibrary.com.]

TABLE V. 1H-MRS of NAA/Cr and Cho/Cr of left centrum semiovale in the CT group (n = 17) and the no-CT group (n = 14)

	CT group (n = 17)	No-CT group (n = 14)	Increase/ Decrease	P value
NAA	8.79 ± 0.62	9.19 ± 0.63	−4.4%	0.10
Cr	5.31 ± 0.33	5.13 ± 0.42	+3.5%	0.20
Cho	1.83 ± 0.25	1.85 ± 0.21	−1.1%	0.87
NAA/Cr	1.66 ± 0.13	1.80 ± 0.15	−7.8%	0.01
Cho/Cr	0.35 ± 0.05	0.36 ± 0.06	−2.9%	0.37

Absolute values are expressed in institutional units.
1H-MRS, Proton MR spectroscopy; CT, chemotherapy; NAA, the sum of *N*-acetylaspartate + *N*-acetylaspartylglutamate (NAAG); Cr, creatine; Cho, choline, the sum of the glycerophosphoryl-choline and phosphocholine.

showing BOLD hypoactivation in lateral posterior parietal cortex (Fig. 2).

VBM and fMRI

VBM showed reductions of gray matter volume in the CT versus the no-CT group in posterior parts of the brain: left lateral posterior parietal cortex, bilateral precuneus, left occipital cortex and bilateral cerebellum (predominantly left hemisphere). No increases of gray matter volume were found for the CT versus the no-CT group. To compare VBM data with results of our previous fMRI study, the VBM map reflecting decreases in gray matter volume in the CT versus to no-CT group were overlaid on the BOLD contrast images reflecting relatively decreased activation in the CT versus the no-CT group during the encoding phase of a paired associates memory test. The reduction in gray matter volume as measured with VBM overlapped with the hypoactive area in left lateral posterior parietal cortex as measured with fMRI. The hypoactive area in right lateral posterior parietal cortex, however, did not show a volume reduction (Fig. 3).

Correlations of DTI Parameters with NAA/Cr and NAA

For correlation of DTI with 1H-MRS, first, a region-of-interest (ROI) approach was used. For mean DTI values within the 1H-MRS voxel, in the CT group significant negative correlations were found for MD and RD with NAA/Cr ($r = -0.48$ and $r = -0.50$, respectively). AD did not correlate significantly with NAA/Cr ($r = -0.40$). MD, AD, and RD correlated significantly with absolute NAA ($r = -0.61$, $r = -0.59$, and $r = -0.58$, respectively) in the CT group (Fig. 4). In the CT group, TBSS revealed a significant negative correlation of MD with NAA/Cr in the left centrum semiovale and mainly superiorly located white matter regions: bilateral superior and posterior corona radiata, bilateral superior longitudinal fasciculus, and left retrolenticular part of the internal capsule ($r = -0.74$). No significant correlations were found for the no-CT group.

Correlations of DTI Parameters with Cognitive Test Performance

No significant correlations were found of MD with cognitive test indices. However, when lowering the statistic

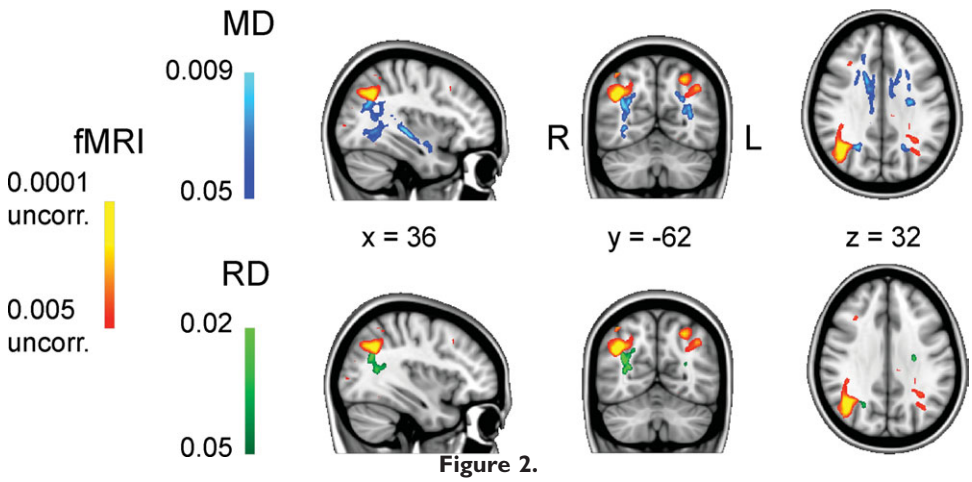

Figure 2.

Group differences for DTI and fMRI. Increases in mean diffusivity (MD) and radial diffusivity (RD, upper and lower panel, respectively) for the chemotherapy (CT) versus the no-CT group in white matter tracts (posterior thalamic/optic radiation) are colocalized with hypoactivation in bilateral posterior parietal cortex for the CT compared to the no-CT group during a paired associates task [de Ruiter et al., 2011]. All images are overlaid on the MNI152-template. For DTI, cluster-based thresholding at $P < 0.05$ was applied, fully corrected for multiple comparisons. Significant MD and RD clusters have been thickened for ease of visualization. Color bars show range of uncorrected (fMRI) and corrected (MD and RD) P values. [Color figure can be viewed in the online issue, which is available at wileyonlinelibrary.com.]

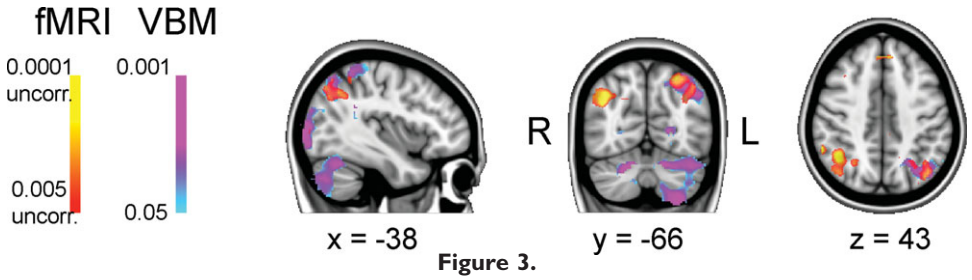

Figure 3.

Group differences for voxel-based morphometry (VBM) and fMRI. Decreased regional gray matter volume in the chemotherapy (CT) group compared with the no-CT group, as assessed with VBM, overlaps with fMRI hypoactivation during a paired associates task [de Ruiter et al., 2011] in left posterior parietal cortex. Right posterior parietal cortex only shows hypoactivation but no volume reduction. Also, volume reductions can be discerned in bilateral cerebellum (stronger in the left than in the right hemisphere). Color bars show range of corrected (VBM) and uncorrected (fMRI) *P* values. [Color figure can be viewed in the online issue, which is available at wileyonlinelibrary.com.]

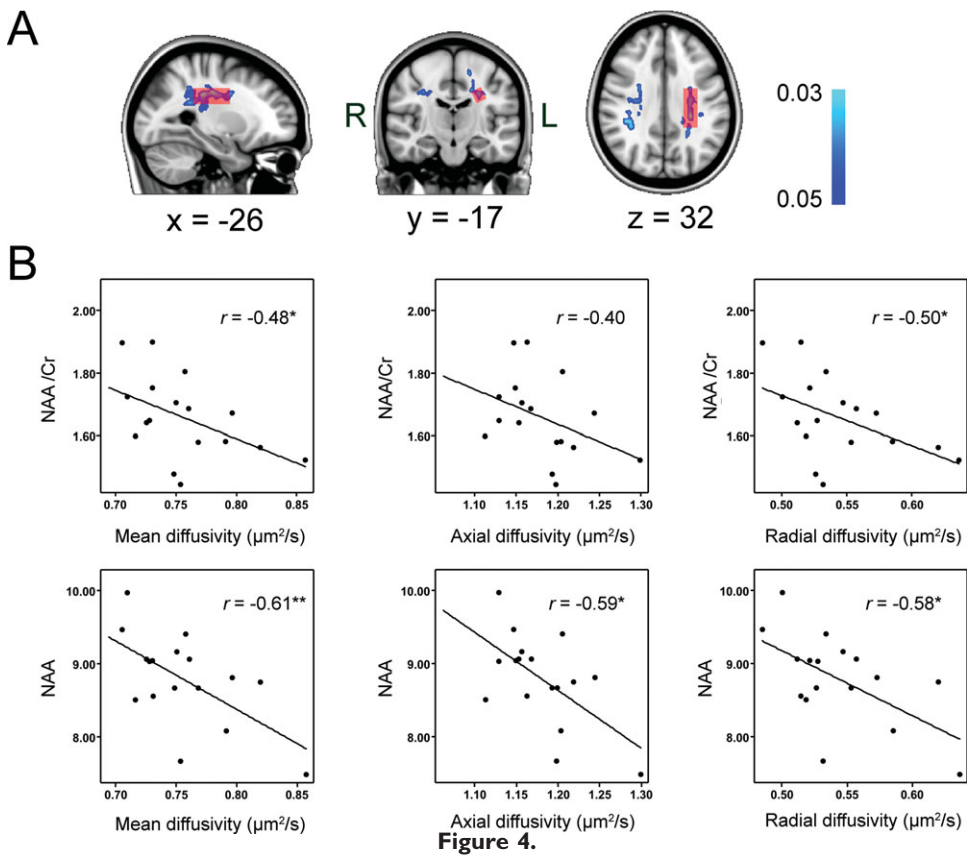

Figure 4.

Correlations of DTI values with single voxel proton MR spectroscopy (1H-MRS) in the chemotherapy (CT) group. 1H-MRS was performed in the left centrum semiovale (white matter). **A**: The approximate location of the voxel is shown in red on the MNI-152 template (upper panel). Mean diffusivity (MD) values for skeletonized white matter were correlated with NAA and NAA/Cr. We also used tract-based spatial statistics (TBSS) with cluster-based thresholding at $P < 0.05$, fully corrected for multiple comparisons. Clusters showing a significant negative correlation with NAA/Cr are overlaid on the MNI-152 template. Significant clusters have been thickened for ease of visualization. Color bar shows range of corrected *P* values. **B**: Correlations of mean DTI values of skeletonised white matter within the 1H-MRS voxel. The scatter plots in the upper panels show correlations of MD, axial diffusivity and radial diffusivity with NAA/Cr. The scatter plots in the lower panels show correlations of MD, axial diffusivity and radial diffusivity with NAA (institutional units). $*P < 0.05$, $**P < 0.01$. [Color figure can be viewed in the online issue, which is available at wileyonlinelibrary.com.]

threshold to $P < 0.1$ corrected, we found a marginally significant negative correlation between MD and Flanker test performance in the CT group in the anterior limb of the internal capsule, the external capsule and the anterior corona radiata (right hemisphere, Supplementary Fig. 1).

DISCUSSION

This comprehensive study is the first to show that, almost 10 years after treatment, adjuvant systemic treatment with high-dose chemotherapy given to patients at risk for recurrence of breast cancer is associated with detrimental effects on brain morphology and function as measured with DTI, 1H-MRS, fMRI, VBM, and neurocognitive tests. Macroscopically, on visual inspection according to Fazekas ratings white matter did not differ between the CT group and the no-CT group. However, on a microscopic level using advanced neuroimaging tools, we observed the following imaging abnormalities in the CT group relative to the no-CT group: (1) a mean increase in MD, AD, and RD across the entire white matter skeleton, (2) focal decreases in FA and increases in MD and RD in white matter tracts relevant for cognitive functioning, (3) a reduction of NAA/Cr in cerebral white matter (left centrum semiovale). More importantly, DTI increases of MD and RD in white matter colocalized with a reduction of gray matter volume and fMRI hypoactivation in posterior parietal areas. Also, diffusivity values correlated negatively with NAA and NAA/Cr only in the CT group. We elaborate on these findings below.

A significant increase of mean MD was observed in the CT versus no-CT group. Also, AD and RD showed significant increases, suggesting that the increase in MD was driven by increases in both AD and RD. This might also explain why mean FA was not significantly decreased: when diffusivity increases both parallel and perpendicular to white matter tracts, directional diffusivity will not increase. Animal studies have shown that acute axonal injury is associated with AD *decrease* [Song et al., 2003]. Although less consistent than findings on RD, a growing number of studies in various neurodegenerative diseases (including aging) points to an *increase* in AD, which, like in our study, is usually less pronounced than the increase in RD [Acosta-Cabronero et al., 2010; Della Nave et al., 2010, 2011; Rosas et al., 2010; Salat et al., 2010; Sullivan et al., 2010]. Increased AD might result from an expansion of extra-axonal space due to reduced axonal size, which would allow faster water movement along axons [Rosas et al., 2010]. If we assume that AD and RD reflect axonal injury and demyelination, respectively, these findings indicates that high-dose CT is associated with both types of white matter injury.

In addition to these changes in mean AD and RD across the white matter skeleton, we observed regional decreases in FA, and/or increases in MD and RD in a number of white matter tracts of the CT group using TBSS [for instance, external capsule, sagittal stratum (including the inferior longitudinal and inferior fronto-occipital fasciculus), posterior thalamic radiation, and several subregions of corona radiata]. The majority of these regions have been implicated in cognitive functioning [Schmahmann et al., 2008].

Our results corroborate the findings of Deprez and coworkers, who also reported widespread reductions in FA and increases in MD in breast cancer patients that received a standard-dose adjuvant regimen (FEC and Paclitaxel) followed by tamoxifen. In this study, patients were examined within 6 months after completion of chemotherapy [Deprez et al., 2011]. Overlap in affected white matter areas between Deprez's and our study include the sagittal stratum, superior longitudinal fasciculus, corpus callosum, and superior corona radiata. Future studies will have to reveal whether this specific chemotherapeutic regimen is also associated with long-term effects like we observed in the present study.

1H-MRS in the left centrum semiovale (covering parts of the superior and posterior corona radiata and the superior longitudinal fasciculus) showed a 7.8% decrease in NAA/Cr of the CT group relative to the no-CT group, in the absence of changes in Cho. As NAA is localized almost exclusively in neurons, the reduction in relative NAA in the centrum semiovale suggests that axonal degeneration contributed to the observed diffusion abnormalities. The inverse correlation of NAA with MD, AD, and RD in the CT group suggests that lower axonal viability is associated with higher diffusivity of water both parallel and perpendicular to axons. The absence of Cho increases in the CT group is perhaps not surprising, as it is only found during active myelin breakdown, and in a disease like multiple sclerosis typically returns to normal over months [De Stefano et al., 1995]. 1H-MRS assessments earlier after treatment may be helpful to demonstrate chemotherapy induced acute demyelination (increase in Cho). Like in multiple sclerosis, axonal degeneration may be primary or secondary to demyelination as result of a lack of myelin-associated trophic factors [Bitsch et al., 2000; Trapp et al., 1999], almost 10 years after administration of chemotherapy.

Multimodal MRI imaging also allowed us to compare detrimental effects of chemotherapy on white and gray matter. Interestingly, bilateral increases in MD in the posterior thalamic radiation were located adjacent to fMRI hypoactivations in bilateral posterior parietal cortex that we reported in a previous study in the same group [de Ruiter et al., 2011]. These hypoactivations were found during a memory encoding test and a visuospatial planning test. Moreover, a region in left posterior parietal cortex, overlapping with the fMRI data, showed a reduction in gray matter volume for the CT relative to the no-CT group. It therefore appears that in the currently studied group, high-dose chemotherapy is associated with long-term detrimental effects particularly on parietal cortex and adjacent white matter tracts that might (partly) underlie impaired cognitive functioning in the CT group. Future

studies are needed to further elucidate the relation of reductions in white matter quality and adjacent gray matter volume reductions and aberrant brain activation patterns.

We found a marginally significant negative correlation of MD with Flanker test performance in the CT group in the anterior limb of the internal capsule, the external capsule and the anterior corona radiata, all white matter regions that are implicated in cognitive functioning [Schmahmann et al., 2008]. Particularly interesting is the correlation of MD in the anterior limb of the internal capsule with performance: this region connects to the cingulate cortex [Schmahmann et al., 2008], that is considered a key brain region in monitoring response conflicts as elicited by the Flanker test [van Veen and Carter, 2002].

Our findings are thus indicative for an association between high-dose chemotherapy and long-term demyelination and axonal injury. Preclinical studies have shown that 5-FU, one of the agents in FEC, acutely damages myelin sheets and myelin precursors in vivo and in vitro [Dietrich et al., 2006; Han et al., 2008]. Currently, it is unknown whether some white matter tracts are more vulnerable than others to chemotherapy (as suggested by the TBSS analysis), and which chemotherapeutic regimens are particularly harmful to the brain. It is particularly worth mentioning in this respect, that the high-dose CT administered to cancer survivors in the present study is a very intense treatment that is not longer commonly used for the treatment of breast cancer (although high-dose regimens are used for the treatment of other cancers). Before high-dose CT was given, harvesting of progenitor cells took place to prevent these cells from being destroyed by CT. After high-dose CT administration, these cells were returned to the bloodstream (autologous progenitor cell transplantation).

Some limitations of the present study should be noted. All participants in the CT-group were treated with tamoxifen for almost four years on average, compared to only one from the no-CT group. Tamoxifen treatment has been associated with impaired cognitive function and imaging abnormalities [Eberling et al., 2004; Schilder et al., 2010a] and might have contributed to the present findings. However, when compared to cancer survivors that received standard-dose chemotherapy and tamoxifen, it was shown in a previous study by our group that high-dose CT was still associated with higher rates of cognitive impairment [Schagen et al., 2006]. Moreover, in the Deprez et al. study rates of tamoxifen use were similar in the CT and no-CT group. Therefore, it is not likely that tamoxifen use is largely or solely responsible for our findings. Another limitation of the present study is its cross-sectional design. Several investigators have shown impaired cognitive functioning and functional imaging abnormalities before the start of treatment in breast cancer patients [Ahles et al., 2008; Cimprich et al., 2010; Schilder et al., 2010b]. As a consequence, we cannot exclude that our group differences were pre-existent to some extent. Thus, future studies will have to address whether standard-dose adjuvant systemic treatment has a similar detrimental effect on brain structure and function, which is the contribution of hormonal treatment, and whether predisposing factors contribute to brain abnormalities.

CONCLUSION

We present evidence for long-term detrimental effects on brain white and gray matter likely induced by high-dose adjuvant chemotherapy, with subsequent impingement on cognitive function. Using a multimodality imaging approach we provide insight in the pathophysiology of the neurotoxic effects of cytotoxic agents on the living human brain.

ACKNOWLEDGMENT

The authors thank Emiel Rutgers and Marie-Jeanne Vrancken Peeters for their help in patient recruitment.

REFERENCES

Aaronson NK, Ahmedzai S, Bergman B, Bullinger M, Cull A, Duez NJ, Filiberti A, Flechtner H, Fleishman SB, de Haes JC (1993): The European organization for research and treatment of cancer QLQ-C30: A quality-of-life instrument for use in international clinical trials in oncology. J Natl Cancer Inst 85:365–376.

Abraham J, Haut MW, Moran MT, Filburn S, Lemieux S, Kuwabara H (2008): Adjuvant chemotherapy for breast cancer: Effects on cerebral white matter seen in diffusion tensor imaging. Clin Breast Cancer 8:88–91.

Acosta-Cabronero J, Williams GB, Pengas G, Nestor PJ (2010): Absolute diffusivities define the landscape of white matter degeneration in Alzheimer's disease. Brain 133:529–539.

Ahles TA, Saykin AJ (2007): Candidate mechanisms for chemotherapy-induced cognitive changes. Nat Rev Cancer 7:192–201.

Ahles TA, Saykin AJ, McDonald BC, Furstenberg CT, Cole BF, Hanscom BS, Mulrooney TJ, Schwartz GN, Kaufman PA (2008): Cognitive function in breast cancer patients prior to adjuvant treatment. Breast Cancer Res Treat 110:143–152.

Bitsch A, Schuchardt J, Bunkowski S, Kuhlmann T, Bruck W (2000): Acute axonal injury in multiple sclerosis. Correlation with demyelination and inflammation. Brain 123:1174–1183.

Brown MS, Simon JH, Stemmer SM, Stears JC, Scherzinger A, Cagnoni PJ, Jones RB (1995): MR and proton spectroscopy of white matter disease induced by high-dose chemotherapy with bone marrow transplant in advanced breast carcinoma. AJNR Am J Neuroradiol 16:2013–2020.

Brown MS, Stemmer SM, Simon JH, Stears JC, Jones RB, Cagnoni PJ, Sheeder JL (1998): White matter disease induced by high-dose chemotherapy: Longitudinal study with MR imaging and proton spectroscopy. AJNR Am J Neuroradiol 19: 217–221.

Budde MD, Xie M, Cross AH, Song SK (2009): Axial diffusivity is the primary correlate of axonal injury in the experimental autoimmune encephalomyelitis spinal cord: A quantitative pixelwise analysis. J Neurosci 29:2805–2813.

Cimprich B, Reuter-Lorenz P, Nelson J, Clark PM, Therrien B, Normolle D, Berman MG, Hayes DF, Noll DC, Peltier S, Welsh RC (2010): Prechemotherapy alterations in brain function in women with breast cancer. J Clin Exp Neuropsychol 32:324–331.

Correa DD, Ahles TA (2008): Neurocognitive changes in cancer survivors. Cancer J 14:396–400.

de Ruiter MB, Reneman L, Boogerd W, Veltman DJ, van Dam FS, Nederveen AJ, Boven E, Schagen SB (2011): Cerebral hyporesponsiveness and cognitive impairment 10 years after chemotherapy for breast cancer. Hum Brain Mapp 32:1206–1219.

De Stefano N, Matthews PM, Antel JP, Preul M, Francis G, Arnold DL (1995): Chemical pathology of acute demyelinating lesions and its correlation with disability. Ann Neurol 38:901–909.

Della Nave R, Ginestroni A, Diciotti S, Salvatore E, Soricelli A, Mascalchi M (2011): Axial diffusivity is increased in the degenerating superior cerebellar peduncles of Friedreich's ataxia. Neuroradiology 53:367–372.

Della Nave R, Ginestroni A, Tessa C, Giannelli M, Piacentini S, Filippi M, Mascalchi M (2010): Regional distribution and clinical correlates of white matter structural damage in Huntington disease: A tract-based spatial statistics study. AJNR Am J Neuroradiol 31:1675–1681.

Deprez S, Amant F, Yigit R, Porke K, Verhoeven J, Van den SJ, Smeets A, Christiaens MR, Leemans A, Van HW, Vandenberghe J, Vandenbulcke M, Sunaert S (2011): Chemotherapy-induced structural changes in cerebral white matter and its correlation with impaired cognitive functioning in breast cancer patients. Hum Brain Mapp 32:480–493.

Dietrich J, Han R, Yang Y, Mayer-Proschel M, Noble M (2006): CNS progenitor cells and oligodendrocytes are targets of chemotherapeutic agents in vitro and in vivo. J Biol 5:22.

Eberling JL, Wu C, Tong-Turnbeaugh R, Jagust WJ (2004): Estrogen- and tamoxifen-associated effects on brain structure and function. Neuroimage 21:364–371.

Fazekas F, Chawluk JB, Alavi A, Hurtig HI, Zimmerman RA (1987): MR signal abnormalities at 1.5 T in Alzheimer's dementia and normal aging. AJR Am J Roentgenol 149:351–356.

Han R, Yang YM, Dietrich J, Luebke A, Mayer-Proschel M, Noble M (2008): Systemic 5-fluorouracil treatment causes a syndrome of delayed myelin destruction in the central nervous system. J Biol 7:12.

Hesbacher PT, Rickels K, Morris RJ, Newman H, Rosenfeld H (1980): Psychiatric illness in family practice. J Clin Psychiatry 41:6–10.

Inagaki M, Yoshikawa E, Matsuoka Y, Sugawara Y, Nakano T, Akechi T, Wada N, Imoto S, Murakami K, Uchitomi Y (2007): Smaller regional volumes of brain gray and white matter demonstrated in breast cancer survivors exposed to adjuvant chemotherapy. Cancer 109:146–156.

Kesler SR, Bennett FC, Mahaffey ML, Spiegel D (2009): Regional brain activation during verbal declarative memory in metastatic breast cancer. Clin Cancer Res 15:6665–6673.

Mangin JF, Poupon C, Clark C, Le Bihan D, Bloch I (2002): Distortion correction and robust tensor estimation for MR diffusion imaging. Med Image Anal 6:191–198.

McDonald BC, Conroy SK, Ahles TA, West JD, Saykin AJ (2010): Gray matter reduction associated with systemic chemotherapy for breast cancer: A prospective MRI study. Breast Cancer Res Treat 123:819–828.

Mignone RG, Weber ET (2006): Potent inhibition of cell proliferation in the hippocampal dentate gyrus of mice by the chemotherapeutic drug thioTEPA. Brain Res 1111:26–29.

Mori S, Oishi K, Jiang H, Jiang L, Li X, Akhter K, Hua K, Faria AV, Mahmood A, Woods R, Toga AW, Pike GB, Neto PR, Evans A, Zhang J, Huang H, Miller MI, van ZP, Mazziotta J (2008): Stereotaxic white matter atlas based on diffusion tensor imaging in an ICBM template. Neuroimage 40:570–582.

Nichols TE, Holmes AP (2002): Nonparametric permutation tests for functional neuroimaging: A primer with examples. Hum Brain Mapp 15:1–25.

Pierpaoli C, Basser PJ (1996): Toward a quantitative assessment of diffusion anisotropy. Magn Reson Med 36:893–906.

Pierpaoli C, Jezzard P, Basser PJ, Barnett A, Di CG (1996): Diffusion tensor MR imaging of the human brain. Radiology 201:637–648.

Provencher SW (1993): Estimation of metabolite concentrations from localized in vivo proton NMR spectra. Magn Reson Med 30:672–679.

Rosas HD, Lee SY, Bender AC, Zaleta AK, Vangel M, Yu P, Fischl B, Pappu V, Onorato C, Cha JH, Salat DH, Hersch SM (2010): Altered white matter microstructure in the corpus callosum in Huntington's disease: Implications for cortical "disconnection." Neuroimage 49:2995–3004.

Sakane T, Yamashita S, Yata N, Sezaki H (1999): Transnasal delivery of 5-fluorouracil to the brain in the rat. J Drug Target 7:233–240.

Salat DH, Tuch DS, van der Kouwe AJ, Greve DN, Pappu V, Lee SY, Hevelone ND, Zaleta AK, Growdon JH, Corkin S, Fischl B, Rosas HD (2010): White matter pathology isolates the hippocampal formation in Alzheimer's disease. Neurobiol Aging 31:244–256.

Schagen SB, Muller MJ, Boogerd W, Mellenbergh GJ, van Dam FS (2006): Change in cognitive function after chemotherapy: A prospective longitudinal study in breast cancer patients. J Natl Cancer Inst 98:1742–1745.

Schagen SB, van Dam FS, Muller MJ, Boogerd W, Lindeboom J, Bruning PF (1999): Cognitive deficits after postoperative adjuvant chemotherapy for breast carcinoma. Cancer 85:640–650.

Schagen SB, Vardy J (2007): Cognitive dysfunction in people with cancer. Lancet Oncol 8:852–853.

Schilder CM, Seynaeve C, Beex LV, Boogerd W, Linn SC, Gundy CM, Huizenga HM, Nortier JW, van de Velde CJ, van Dam FS, Schagen SB (2010a): Effects of tamoxifen and exemestane on cognitive functioning of postmenopausal patients with breast cancer: Results from the neuropsychological side study of the tamoxifen and exemestane adjuvant multinational trial. J Clin Oncol 28:1294–1300.

Schilder CM, Seynaeve C, Linn SC, Boogerd W, Beex LV, Gundy CM, Nortier JW, van de Velde V, van Dam FS, Schagen SB (2010b): Cognitive functioning of postmenopausal breast cancer patients before adjuvant systemic therapy, and its association with medical and psychological factors. Crit Rev Oncol Hematol 76:133–141.

Schmahmann JD, Smith EE, Eichler FS, Filley CM (2008): Cerebral white matter: Neuroanatomy, clinical neurology, and neurobehavioral correlates. Ann N Y Acad Sci 1142:266–309.

Schmand B, Lindeboom J, van Harskamp F. 1992. De Nederlandse Leestest voor Volwassenen. Lisse: Swets & Zeitlinger.

Seigers R, Pourtau L, Schagen SB, van Dam FS, Koolhaas JM, Konsman JP, Buwalda B (2010): Inhibition of hippocampal cell proliferation by methotrexate in rats is not potentiated by the presence of a tumor. Brain Res Bull 81:472–476.

Seigers R, Schagen SB, Beerling W, Boogerd W, van Tellingen O, van Dam FS, Koolhaas JM, Buwalda B (2008): Long-lasting

suppression of hippocampal cell proliferation and impaired cognitive performance by methotrexate in the rat. Behav Brain Res 186:168–175.

Seigers R, Schagen SB, Coppens CM, van der Most PJ, van Dam FS, Koolhaas JM, Buwalda B (2009): Methotrexate decreases hippocampal cell proliferation and induces memory deficits in rats. Behav Brain Res 201:279–284.

Shilling V, Jenkins V (2007): Self-reported cognitive problems in women receiving adjuvant therapy for breast cancer. Eur J Oncol Nurs 11:6–15.

Silverman DH, Dy CJ, Castellon SA, Lai J, Pio BS, Abraham L, Waddell K, Petersen L, Phelps ME, Ganz PA (2007): Altered frontocortical, cerebellar, and basal ganglia activity in adjuvant-treated breast cancer survivors 5–10 years after chemotherapy. Breast Cancer Res Treat 103:303–311.

Smith SM, Jenkinson M, Johansen-Berg H, Rueckert D, Nichols TE, Mackay CE, Watkins KE, Ciccarelli O, Cader MZ, Matthews PM, Behrens TE (2006): Tract-based spatial statistics: Voxelwise analysis of multi-subject diffusion data. Neuroimage 31:1487–1505.

Smith SM, Jenkinson M, Woolrich MW, Beckmann CF, Behrens TE, Johansen-Berg H, Bannister PR, De LM, Drobnjak I, Flitney DE, Niazy RK, Saunders J, Vickers J, Zhang Y, De Stefano N, Brady JM, Matthews PM (2004): Advances in functional and structural MR image analysis and implementation as FSL. Neuroimage 23 (Suppl 1):S208–S219.

Song SK, Sun SW, Ju WK, Lin SJ, Cross AH, Neufeld AH (2003): Diffusion tensor imaging detects and differentiates axon and myelin degeneration in mouse optic nerve after retinal ischemia. Neuroimage 20:1714–1722.

Song SK, Sun SW, Ramsbottom MJ, Chang C, Russell J, Cross AH (2002): Dysmyelination revealed through MRI as increased radial (but unchanged axial) diffusion of water. Neuroimage 17:1429–1436.

Song SK, Yoshino J, Le TQ, Lin SJ, Sun SW, Cross AH, Armstrong RC (2005): Demyelination increases radial diffusivity in corpus callosum of mouse brain. Neuroimage 26:132–140.

Stemmer SM, Stears JC, Burton BS, Jones RB, Simon JH (1994): White matter changes in patients with breast cancer treated with high-dose chemotherapy and autologous bone marrow support. AJNR Am J Neuroradiol 15:1267–1273.

Strong JM, Collins JM, Lester C, Poplack DG (1986): Pharmacokinetics of intraventricular and intravenous *N*,*N*′,*N*″-triethylenethiophosphoramide (thiotepa) in rhesus monkeys and humans. Cancer Res 46:6101–6104.

Sullivan EV, Rohlfing T, Pfefferbaum A (2010): Quantitative fiber tracking of lateral and interhemispheric white matter systems in normal aging: Relations to timed performance. Neurobiol Aging 31:464–481.

Sun SW, Liang HF, Cross AH, Song SK (2008): Evolving Wallerian degeneration after transient retinal ischemia in mice characterized by diffusion tensor imaging. Neuroimage 40:1–10.

Sun SW, Liang HF, Trinkaus K, Cross AH, Armstrong RC, Song SK (2006): Noninvasive detection of cuprizone induced axonal damage and demyelination in the mouse corpus callosum. Magn Reson Med 55:302–308.

Trapp BD, Ransohoff RM, Fisher E, Rudick RA (1999): Neurodegeneration in multiple sclerosis: relationship to neurological disability. The Neuroscientist 5:48–57.

van Dam FS, Schagen SB, Muller MJ, Boogerd W, vd Wall E, Droogleever Fortuyn ME, Rodenhuis S (1998): Impairment of cognitive function in women receiving adjuvant treatment for high-risk breast cancer: High-dose versus standard-dose chemotherapy. J Natl Cancer Inst 90:210–218.

van Veen V, Carter CS (2002): The anterior cingulate as a conflict monitor: fMRI and ERP studies. Physiol Behav 77:477–482.

Vardy J, Wefel JS, Ahles T, Tannock IF, Schagen SB (2008): Cancer and cancer-therapy related cognitive dysfunction: An international perspective from the Venice cognitive workshop. Ann Oncol 19:623–629.

Wefel JS, Witgert ME, Meyers CA (2008): Neuropsychological sequelae of non-central nervous system cancer and cancer therapy. Neuropsychol Rev 18:121–131.

Weis J, Poppelreuter M, Bartsch HH (2009): Cognitive deficits as long-term side-effects of adjuvant therapy in breast cancer patients: 'Subjective' complaints and 'objective' neuropsychological test results. Psychooncology 18:775–782.